Dynamic Behaviour of a Flexible Plate behind a Circular Cylinder: Numerical Study on the Effects of Blockage and Cylinder Size

R.K.B. Gallegos[1, 2] and R.N. Sharma[1]

[1]Department of Mechanical Engineering
University of Auckland, Auckland 1142, New Zealand

[2]Institute of Agricultural Engineering
University of the Philippines Los Baños, College, Laguna, 4031, Philippines

Abstract

This paper presents a numerical study on the dynamic behavior of a flexible plate located behind a cylinder and confined between two parallel walls. This two-dimensional fluid-structure interaction problem was performed for four different cylinder sizes, with focus on blockage effects. The oscillation amplitude and frequency of the plate tip were examined as affected by the cylinder size and blockage ratio (ratio of the cylinder diameter to the channel width) which varied from 0.05 to 0.49. The oscillation amplitude and frequency of the plate tip is strongly affected by the combined effects of blockage and cylinder size. The results suggest that the dynamic behaviour of the plate may be altered by varying blockage and cylinder size.

Introduction

The dynamics of a flexible structure attached to a bluff body and immersed in a flow is one of the classical problems in fluid-structure interaction (FSI) analysis. This problem is widely explored in the context of splitter plate analysis [5,6] and heat transfer enhancement in channels [1,8]. However, very few reports on the effects of channel blockage on the oscillation dynamics of a flexible structure seems to be available. The numerical investigations of Lee and You [1] and Furquan and Mittal [2] for example, focused mostly on the dynamics of the elastic structure in an open flow, with little emphasis on blockage effects. Ali et al. [1] and Soti et al. [8] examined such dynamic behaviour in the context of heat transfer enhancement but no extensive investigation on cylinder size and blockage effects were reported. The effects of channel blockage on the flow structure around cylinders are widely reported [14], however, its effects on the dynamic behaviour of the structure attached to the cylinder is not widely established. Such information is useful in various applications like the use of flags as vortex generators for heat transfer enhancement in channels or in between heat fins, where pressure drop and structural oscillations affect thermal performance. This paper presents numerical results on the effects of channel blockage on the oscillation behaviour of a flexible structure attached behind a circular cylinder.

Problem Description

Turek and Hron [12] proposed a benchmark problem for simulating fluid-structure interaction. An elastic structure attached to a rigid cylinder is immersed in a 2D incompressible laminar flow inside a channel (see figure 1).

This paper extends this problem by examining the effects of varying the cylinder diameter d on the oscillation behaviour of the flexible structure located behind the cylinder.
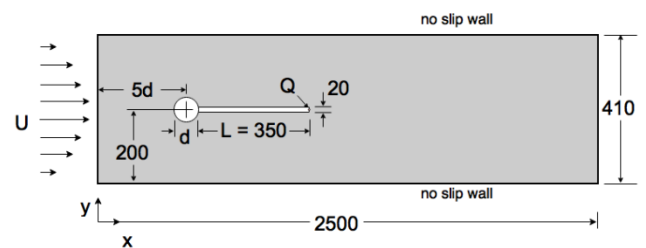
Figure 1. Computational domain for examining the effects of cylinder diameter d on the dynamics of a flexible structure (all dimensions are in millimetres).

Three different variants of this FSI problem were proposed by Turek and Hron depending on the structure and fluid properties. In this study, the FSI2 variant was chosen and the corresponding structure and fluid properties are summarised in table 1.

Properties	Value	Unit
Structure		
Density, ρ_s	10 000	kg/m^3
Poisson's Ratio, ν_s	0.4	-
Elastic Modulus, E	1.4	MPa
Fluid		
Density, ρ_f	1000	kg/m^3
Dynamic viscosity, μ_f	1	Pa-s
Average inlet velocity, (U_{avg})	1	m/s

Table 1. Structural and fluid properties used in the study.

In the present simulations, the cylinder diameter (d) was varied according to table 2. Correspondingly, the blockage ratio (d/H) was varied by varying the cylinder diameter, while maintaining the channel height (H=410 mm) and the location of the cylinder's center (see figure 1). The Reynolds number based on the average inlet velocity and the cylinder diameter (Re_d) were also presented.

Case	d, mm	d/L	d/H	Re_d
1	20	0.06	0.05	20
2	50	0.14	0.12	50
3	100	0.29	0.24	100
4	150	0.43	0.37	150
5	100	0.57	0.49	200

Table 2. Cylinder diameters and dimensionless parameters used in the study.

Numerical Method

Fluid-structure interaction (FSI) involves three numerical challenges: fluid dynamics modeling, structural modeling and deforming mesh challenge. In dealing with most FSI problems, the partitioned solver approach (as opposed to the monolithic approach) is usually employed. In this approach, a dedicated solver is used for each of the fluid, structure, and meshing [3]. In this study, ANSYS Fluent and Mechanical solvers were used for the fluid and structure modeling, respectively. The dynamic meshing feature of ANSYS Fluent took care of the meshing requirements of the problem. These two solvers were strongly-coupled through the ANSYS System coupling feature [3]. A strongly-coupled approach is recommended for large structural displacements which are expected from the structural motions [2].

Modeling unsteady, incompressible fluid flow on a deforming mesh requires that the governing equations be formulated using the Arbitrary Lagrangian-Eulerian (ALE) approach [1,9,13]. In the ALE formulation, the continuity equation may be written as

$$\nabla \cdot u_f = 0 \tag{1}$$

where u_f is the fluid velocity. If $\mathbf{u_m}$ is the mesh velocity, a convective term $(u_f - u_m)$ may be introduced, such that the momentum equation in ALE formulation may be given as

$$\frac{\partial u_f}{\partial t} + \left(u_f - u_m\right) \cdot \nabla u_f = -\frac{\nabla p}{\rho_f} + v_f \nabla^2 u_f \tag{2}$$

where p is the pressure and v_f is the fluid's kinematic viscosity.

For the structure, the Lagrangian formulation is usually employed to describe its motion. An isothermal solid with density ρ_s has the displacement d_s which is given by

$$\rho_s \frac{\partial^2 d_s}{\partial t^2} = \nabla \cdot (S \cdot F^T) + \rho_s f_b \tag{3}$$

where f_b is the body force and F is the deformation gradient tensor given by

$$F = I + \nabla d_s^T \tag{4}$$

where I is the identity and S is the Piola-Kirchoff stress tensor [11]. The Green-Lagrangian strain tensor G given by

$$G = \frac{(F^T \cdot F - I)}{2} \tag{5}$$

is related to S by the following relation:

$$S = 2\mu_s G + \lambda_s \, tr(G) I \tag{6}$$

where tr is the tensor trace and λ_s and μ_s are elastic material Lame constants. In ANSYS Structural, the elastic modulus E and the Poisson ratio v_s are usually specified as inputs and are related to λ_s and μ_s as

$$\lambda_s = \frac{v_s E}{(1+v_s)(1-2v_s)} \tag{7}$$

$$\mu_s = \frac{E}{2(1+v_s)} \tag{8}$$

The motion of the fluid causes pressure and viscous forces to be experienced by the structure. These forces are transmitted at the fluid-structure interface while conditions of equilibrium should be satisfied. At the interface Γ, the following conditions should be satisfied:

$$d_s^\Gamma = d_f^\Gamma \tag{9}$$

$$u_s^\Gamma = u_f^\Gamma \tag{10}$$

$$T_s^\Gamma = -T_f^\Gamma \tag{11}$$

where T^Γ is the traction force at the interface, which is the sum of the pressure and viscous forces.

As the structure moves inside the fluid domain, fluid mesh deforms consequently. ANSYS Fluent features three mesh update methods under its dynamic mesh capability [2]. In this study, only the smoothing and remeshing features were used. The smoothing method is used to adjust the mesh of a zone with a moving or deforming boundary, without changing the number of nodes and their connectivity. This approach ensures that the interior nodes (not the interface nodes) absorb the movement of the interface. In this study, the diffusion smoothing method was employed. In this method, the mesh motion is described by the diffusion equation

$$\nabla \cdot (\gamma \nabla u_m) = 0 \tag{12}$$

where γ is the diffusion coefficient and it can either be a function of the normalized boundary distance r, or the normalized cell volume V, such that

$$\gamma = \frac{1}{r^\alpha} \tag{13}$$

$$\gamma = \frac{1}{V^\alpha} \tag{14}$$

where α is a user input parameter. Equation (13) was the one used in the study with α values from 1 to 1.5. This ensured that during the smoothing, the mesh regions near the boundary were preserved while the regions distant from the boundary absorbed the motion [2].

Simulation Details

Computational Domain, Initial and Boundary Conditions

The dimensions of the fluid domain and the structure are also shown in figure 1. The boundary conditions used for all simulations were all similar to the benchmark conditions by Turek and Hron except for the cylinder diameter. The structure was intentionally situated asymmetrically with respect to the channel height. The walls of the channel and the fluid-structure interface were modelled as non-slip walls. A zero-pressure condition was prescribed at the outlet and the inlet was prescribed with a laminar parabolic velocity profile with the form

$$U(x = 0, y) = \frac{1.5 U_{avg} y(H-y)}{\left(\frac{H}{2}\right)^2} \tag{15}$$

where U_{avg} is the average flow velocity and H is the channel height.

Analysis

The displacement of point Q at the tip of the elastic beam is of particular interest to this problem. All simulations ran until the displacement of point Q at the tip of the elastic structure exhibited a periodic oscillatory behavior. The displacement signals were subjected to Fourier analysis to deduce the dominant frequency f of the oscillation. The oscillation frequency may be conveniently represented by the Strouhal number with respect to the structure length L and average flow velocity, i.e.,

$$St_L = \frac{fL}{U_{avg}} \tag{16}$$

Furthermore, the amplitude A of the oscillation was obtained from the last period of oscillations by applying the formula [12]:

$$A = \frac{max - min}{2} \qquad (17)$$

where **max** and **min** are the maximum and minimum values of point Q positions, respectively.

Mesh Size Sensitivity Test and Solver Validation

Although the general nature of the flow is within the laminar regime, the realizable k-ε turbulence model with enhanced wall treatment was used [2] in all simulations. This is to be able to model the turbulence that is generated within the flow domain. Convergence criteria for all flow and structural quantities were normalised RMS residual targets set of 10^{-6}. A maximum of ten outer coupling iterations was prescribed during the data transfer at the fluid-structure interface, which was sufficient to attain the normalized RMS residual targets of 10^{-4} used for both force and displacement data transfer [3].

The computational domain was extruded in the third dimension by 2 mm and it was discretised using unstructured triangular mesh. In generating the mesh, the focus was given to the vicinity of the fluid-structure interface. After all, the pressure loads coming from the fluid determine the displacements to be exhibited by the structure. In general, the mesh around the structure and the cylinder were refined. Changing the mesh size requires that it should be done in both the structure and fluid domains simultaneously. The mesh size near the FSI interface was largely dictated by the size of the cells in the structure. This was done to prevent errors when the nodes are mapped to the fluid-structure interface. The number of cells in the larger part of the fluid domain (far from the FSI interface) was determined by the global mesh size.

Since only the cylinder size is changed in each case, only the mesh sensitivity test for case 3 (d=100 mm which is similar to Turek and Hron benchmark) is presented here. The different mesh sizes were compared based on the amplitude and frequency of the x and y-displacements of point Q in figure 1. Table 3 summarizes the results of the grid size sensitivity test.

Mesh	No of Elements, Structure	No of Elements, Fluid	Amplitude, mm		Frequency, Hz	
			x	y	x	y
1	237	56,221	12.12	78.40	3.82	1.96
2	485	101,948	12.08	79.05	3.84	1.96
3	1050	267,362	11.92	79.00	3.82	1.96

Table 3. Results of the grid size sensitivity test.

It was decided that Mesh 2 be used in subsequent simulations, a compromise between numerical precision and simulation time. For all the simulations, the time step used was 0.005 s, which was sufficient to examine 100 data points per oscillation cycle.

The results were also validated against published results reported for this FSI case. The validation results are in close agreement with the values reported by Turek and Hron [12] and others [1,4, 8,10]. The values differ to the published results by at most 2.5% and 3.2% for y-oscillation amplitude and frequency, respectively.

Results and Discussion

Fluid-Structure Interaction

Figure 2 shows a glimpse of the dynamic behaviour of the elastic structure taken at four different instances within an oscillation cycle. The benchmark problem (Case 3) is presented here as a representative for the cases. The flow between the cylinder and the walls accelerates, creating regions wherein the pressure at one side of the structure is greater than that at the other side. This pressure differential translates to net forces applied to the structure, which consequently produce structural deformations.
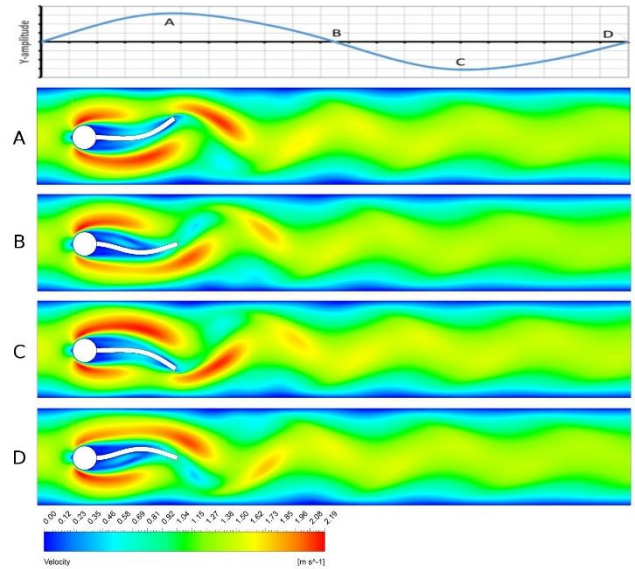
Figure 2. Contours of velocity inside the channel taken at selected time points within one oscillation cycle of the structure's tip.

Effect of Cylinder Diameter and Blockage on Structural Dynamics

The time required to reach steady-state oscillations vary depending on the mast size. Respectively, d/H = 0.05, 0.12, 0.04, 0.37 and 0.49 took about 65 s, 25 s, 7.5 s, 11.5 s, 35 s of flow-time for the structure to reach steady state oscillations. Figure 3 shows the oscillation behaviour of the structure and the flow at its immediate vicinity. The oscillation dynamics of the flexible structure was largely affected by the cylinder size and blockage. The observed oscillation shape is similar for all the cases, characterized by a bell-shaped, single-neck oscillation mode. In general, more stable structure is observed as mast size and blockage decreased.
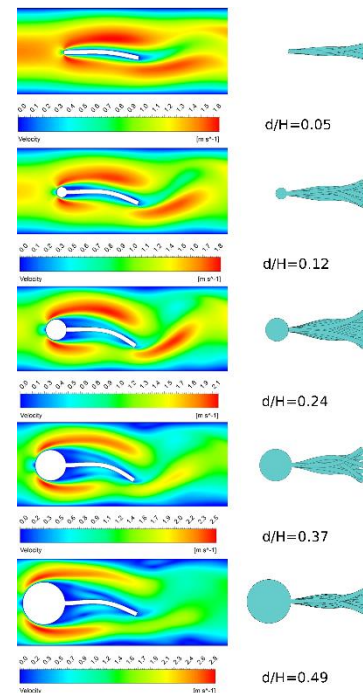
Figure 3. Flow velocity around the structure taken when the tip is at its lowest position (left) and superimposed oscillation shapes (right) for different d/H cases.

For all cases, the oscillation frequency of the tip of the structure is higher in the streamwise (x) direction than in the spanwise (y) direction. However, the y-amplitude is higher than the x-amplitude. For d/H<0.24, the oscillation frequency and amplitude, for both x and y directions, increased with increasing cylinder diameter or blockage ratio (figure 4). At higher blockage ratios, A/L decreased and St_L slightly increased or were essentially unchanged.
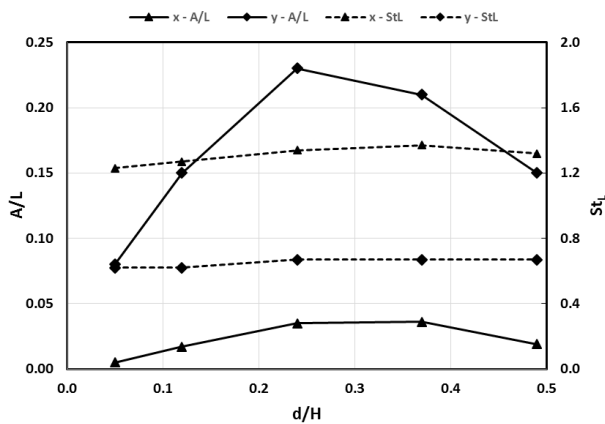
Figure 4. Oscillation amplitude (A/L) and tip oscillation Strouhal number (St_L) of the structure at various blockage ratios (d/H).

In the context of a cylinder in cross flow, most of the cases examined (at Re_d = 50-150) lie in a regime where the flow is characterised by periodic vortex or eddy shedding from the cylinder. This periodic shedding of vortices (see figure 2) translated to a periodic regions of pressure gradients at the wake of the cylinder and either side of the structure, creating net forces that caused structural deformation. Thus, the frequency of vortex shedding from the mast primarily governed the observed dynamics of the structure. In the case of d/H=0.05, the size of the mast is equal to the structure thickness, and vortex shedding form the mast alone played a less significant role on the oscillation. Rather, the observed oscillation is attributed primarily to the periodic shedding of the structure as a whole, aided by inherent pressure gradient across the structure which is located at an offset with respect to the centre of the channel.

Vortex shedding frequency increases with increasing blockage ratio [7,14]. In particular, solid blockage increases velocity around the cylinder, creating more vorticity and stronger eddies. This effect was evident in the streamwise (x-direction) tip oscillation of the structure, which shows slightly increasing amplitude and frequency as blockage was increased.

Blockage also narrowed the near wake of the cylinder, thus increasing the vortex shedding frequency [14]. This effect is also manifested on the lower amplitude and almost similar frequency of cases where d/H>0.24. The narrowing of the wake along the spanwise (y) direction of the channel (see figure 3) at d/H>0.24 produced tip amplitudes which are lower than the observed amplitudes at d/H=0.24. In addition, larger cylinder diameters produced larger regions with low velocity and pressure gradients across the structure, translating to lower oscillation amplitudes. For the same structure length, it seems that there is an optimum blockage ratio in which the spanwise tip oscillation is maximised, since lower amplitudes and frequencies were also observed for smaller cylinder diameters.

Conclusions

This study aimed to determine the effects of channel blockage on the oscillation behaviour of a flexible structure behind a circular cylinder. The blockage was varied by varying the cylinder size as the channel width was maintained. In all cases examined, the tip oscillation amplitude in the streamwise (x) direction is lower than

the spanwise (y) direction. However, the x-oscillation showed higher frequency than the y-oscillation. Simulations further revealed that blockage, as in the case of bare cylinders, increased the vortex shedding frequency of the cylinder and the walls confined the flow at cylinder wake. For the same structure length, there is an optimum blockage to maximise the oscillation frequency and amplitude of the elastic structure behind the cylinder.

References

[1] Ali, S., Habchi, C., Menanteau, S., Lemenand, T., & Harion, J. Heat Transfer and Mixing Enhancement by Free Elastic Flaps Oscillation. *International Journal of Heat and Mass Transfer, 85*, 2015, 250-264.

[2] ANSYS Inc. *ANSYS 16.0 Documentation - Fluent User's Guide* SAS IP Inc, 2014a.

[3] ANSYS Inc. *ANSYS 16.0 Documentation - System Coupling User's Guide* SAS IP Inc, 2014b.

[4] Bhardwaj, Rajneesh, and Rajat Mittal. Benchmarking a Coupled Immersed-Boundary-Finite-Element Solver for Large-Scale Flow-Induced Deformation." *AIAA Journal* 50(7), 2012, 1638-42

[5] Furquan, M., & Mittal, S. Flow Past Two Square Cylinders with Flexible Splitter Plates. *Computational Mechanics, 55*(6), 2015, 1155-1166.

[6] Lee, J., & You, D. Study of Vortex-Shedding-Induced Vibration of a Flexible Splitter Plate behind a Cylinder. *Physics of Fluids (1994-Present), 25*(11), 2013, 110811.

[7] Patil, P. P., & Tiwari, S. Effect of Blockage Ratio on Wake Transition for Flow Past Square Cylinder. *Fluid Dynamics Research, 40*(11), 2008, 753-778.

[8] Soti, A. K., Bhardwaj, R., & Sheridan, J. Flow-Induced Deformation of a Flexible Thin Structure as Manifestation of Heat Transfer Enhancement. *International Journal of Heat and Mass Transfer, 84*, 2015, 1070-1081.

[9] Souli, M., Ouahsine, A., & Lewin, L. ALE Formulation for Fluid–Structure Interaction Problems. *Computer Methods in Applied Mechanics and Engineering, 190*(5), 2000, 659-675.

[10] Tian, F., Dai, H., Luo, H., Doyle, J. F., & Rousseau, B. Fluid–Structure Interaction Involving Large Deformations: 3D Simulations and Applications to Biological Systems. *Journal of Computational Physics, 258*, 2014, 451-469.

[11] Tuković, Ž, & Jasak, H. Updated lagrangian finite volume solver for large deformation dynamic response of elastic body. *Transactions of FAMENA, 31*(1), 2007.

[12] Turek, S., & Hron, J. Proposal for Numerical Benchmarking of Fluid-Structure Interaction between an Elastic Object and Laminar Incompressible Flow. In H. Bungartz, & M. Schäfer (Eds.), *Fluid-Structure Interaction: Modelling, Simulation, Optimisation*, Springer Berlin Heidelberg, 2006, 371-385.

[13] Wall, W. A., Gerstenberger, A., Gamnitzer, P., Förster, C., & Ramm, E. Large Deformation Fluid-Structure Interaction–Advances in ALE Methods and New Fixed Grid Approaches. *Fluid-Structure Interaction* Springer, 2006, 195-232.

[14] Zdravkovich, M. M. *Flow Around Circular Cylinders : A Comprehensive Guide Through Flow Phenomena, Experiments, Applications, Mathematical Models, and Computer Simulations*. Oxford, Oxford University Press, 1997